Photochemical & Photobiological Sciences

Cite this: *Photochem. Photobiol. Sci.*, 2012, **11**, 1313

www.rsc.org/pps

PAPER

Kasha or state selective behavior in the photochemistry of *ortho*-nitrobenzaldehyde?†

T. Schmierer,[a] G. Ryseck,[a] T. Villnow,[a] N. Regner[b] and P. Gilch*[a]

Received 8th March 2012, Accepted 12th April 2012
DOI: 10.1039/c2pp25057h

The photochemistry of *ortho* nitrobenzaldehyde dissolved in tetrahydrofuran was studied by means of femtosecond UV/Vis and IR spectroscopy. Comparison was made of the spectral and temporal signatures for ~400 nm and ~260 nm excitation. The 400 nm excitation promotes NBA to its lowest excited singlet state of nπ* character whereas for 260 nm an upper excited state of ππ* character is addressed. On the picosecond time scale, the molecule undergoes hydrogen transfer, yielding a ketene intermediate, internal conversion recovering the starting material, and intersystem crossing. Time constants and yields of these processes are virtually not affected by the excitation wavelength. For 400 nm excitation a ~100 fs decay component seen in the 260 nm experiment is absent, indicating that this component is due to a ππ* → nπ* internal conversion. In contrast to its formation, the decay of the ketene intermediate is influenced by the excitation wavelength. This can be attributed to different amounts of vibrational excitation.

1. Introduction

In its stricter formulation Kasha's rule states that luminescence of polyatomic molecules occurs predominately from the lowest excited state of a given multiplicity.[1,2] In the broader sense applied here, Kasha behavior implies that, irrespective of the excitation frequency, a polyatomic molecule will relax to this lowest excited state. Its properties are then decisive for the photo physical and chemical behavior. A corollary of Kasha behavior is the invariance of quantum yields with respect to the excitation frequency (Vavilov's rule[2]). Two arguments rationalize these rules: internal conversion (IC) between upper excited states is faster than IC between the lowest excited state and the ground state. This in turn is attributed to smaller energy gaps between the upper states, which due to the energy gap law[3] results in faster IC processes.[2] Further, vibrational relaxation (intramolecu lar vibrational redistribution (IVR) and vibrational cooling) is assumed to be faster than other processes.

Numerous experiments have shown that vibrational cooling (*i.e.* transfer of vibrational excess energy to the solvent) occurs on the time scale of 1 10 ps for "benzene sized" molecules.[4–6] Many photochemical processes occur with shorter or comparable characteristic times (see *e.g.* ref. 7 and 8). Thus, deviations from Kasha behavior are no surprise. We will here list some examples regarding photochemical behavior but note that deviations con cerning fluorescence emission are textbook knowledge.[2,9] For the *trans* to *cis* isomerisation of azobenzene quantum yields dif fering by a factor of two for excitation of the lowest excited states S_1 (yield equals 0.24 0.31) and S_2 (0.1 0.15) were reported.[10] Notably, femtosecond fluorescence experiments indi cated that excitation of the S_2 state results in quantitative IC to the S_1 state.[10] The authors attribute the different quantum yields to additional vibrational excitation caused by the $S_2 \rightarrow S_1$ tran sition. This excitation seems to promote non reactive decay pro cesses of the S_1 state. Pronounced deviations were also observed for the electrocyclic ring opening of fulgides.[11] A fourfold increase of the quantum yield was reported for a higher excited state in comparison with the lowest. Even addressing different vibrational levels of one electronic state can have an impact on the photochemical yield as demonstrated for the ring opening of chromenes.[12,13]

Here, we will address the photochemistry of *ortho* nitrobenz aldehyde (NBA), the kinetics of which we have studied inten sively during recent years.[14–18] Scheme 1 summarizes a reaction sequence based on these and other studies.[19–21] Singlet excited NBA decays within less than 1 ps *via* three channels: (i) internal conversion partially recovering the starting material, (ii) intra molecular hydrogen transfer resulting in a ketene intermediate, and (iii) intersystem crossing (ISC) populating the triplet state. The triplet state also undergoes hydrogen transfer.[17] This transfer yields a triplet phased bi radical, which upon recombination (~200 ps) contributes to the total amount of ketene formed. The lifetime of this ketene is strongly solvent dependent, ranging from 7 ps in water[21] to 24 ns[20] in dry acetonitrile. For solvents other than water we have shown that the ketene decay results in the formation of a secondary intermediate for which we have suggested a lactone structure.[17,22] This lactone then transforms to the final nitroso product. We could not trace this transformation with our set ups, indicating that it occurs on the time scale of

[a]*Institut für Physikalische Chemie, Heinrich Heine Universität Düsseldorf, Universitätsstr. 1, D 40225 Düsseldorf, Germany. E mail: Peter.Gilch@uni duesseldorf.de; Fax: +49 211 81 12803*
[b]*Fakultät für Physik, Ludwig Maximilians Universität München, Oettingenstr. 67, D 80538 München, Germany*

†Electronic supplementary information (ESI) available. See DOI: 10.1039/c2pp25057h

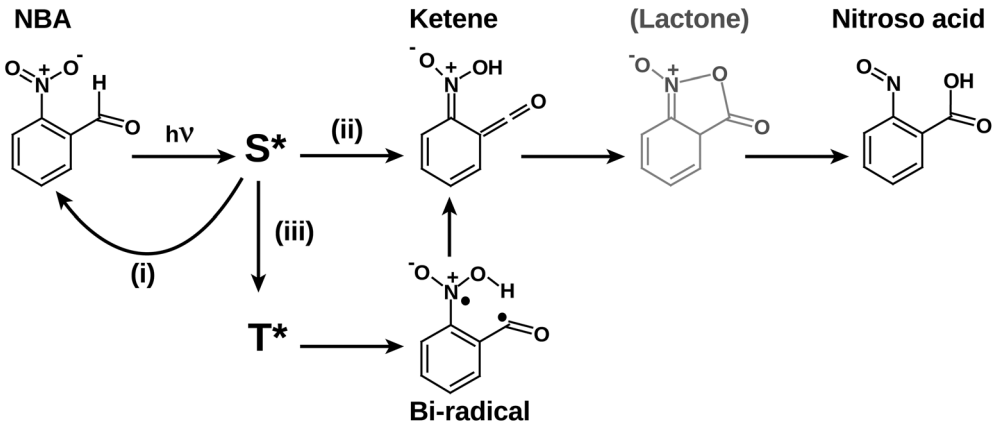

Scheme 1

10 ns or longer. For water as a solvent, the Hamm group[21] recorded data suggesting a direct ketene to nitroso transformation.

The experiments agree upon the ultrafast nature (<1 ps) of the (singlet) hydrogen transfer yielding the ketene. Despite this, NBA seems to obey Kasha's rule rather well. It is long known that the quantum yield of the nitroso formation, which is equal to ~0.5 does only exhibit a weak if any dependence on the excitation frequency.[23,24] Femtosecond fluorescence experiments performed by our group[16] suggest that excitation at ~260 nm, which addresses a higher excited state of ππ* character[25,26] results in ultrafast IC (<100 fs) to a lower lying nπ* state. This IC process is even faster than the hydrogen transfer taking ~500 fs,[14,17] which could explain the Kasha behavior. Indeed, in a recent joint theoretical and experimental study[18] we have compared pathways for ππ* and nπ* excitation. Even though the ππ* state was shown to correlate with the ketene intermediate the potential energy surfaces computed on the MS CASPT2/CASSCF level favor an indirect hydrogen transfer IC to the nπ* state followed by transfer over a direct transfer. For the nπ* state a barrierless path to the ketene was found computationally. Classical dynamics simulation[27] relying on these surfaces indeed favor an efficient hydrogen transfer on the femtosecond timescale for nπ* excitation.

In the aforementioned joint theoretical and experimental study we have briefly compared the femtosecond signatures for the two excitation conditions. Here, we give a more detailed account of the experimental results. Focus will be on three topics: (I) Transition between upper excited states. (II) Impact of the excitation frequency on ISC. (III) Dependence of a secondary process the reaction of the ketene intermediate on the excitation frequency. In the experiments solutions of NBA were excited by ~400 nm and ~260 nm femtosecond laser pulses addressing the lowest nπ* and a ππ* state.[25,26] The resulting spectroscopic changes were probed by UV/Vis and mid IR pulses. The experiments were conducted employing femtosecond laser/amplifier systems operating at slightly different wavelengths (775 810 nm). Excitation light obtained by frequency doubling and tripling of the output of these systems vary accordingly in wavelength. For general purposes we will refer to the two excitation conditions as "blue" (~400 nm) and "UV" (~260 nm). When describing the experiments the exact wavelengths will be given.

2. Experimental

Reaction quantum yields were obtained, relying on laser irradiation and IR spectroscopy. Irradiation and detection were performed in two different flow cells, which were part of a circuit. For irradiation a fused silica flow cell with an optical pathlength of 1 cm was used. The sample solution was stirred during irradiation and a high absorbance (larger than 4 OD) at the excitation wavelength ensured complete absorption of the laser light. The third (355 nm) and fourth (266 nm) harmonic of a Nd:YAG laser (Continuum, NY60) were employed for irradiation. The average power at the sample location was measured with two different powermeters (Coherent, Digi Rad), delivering identical results. After an irradiation interval the solution was pumped into an IR flow cell (BaF_2 windows, path length of 90 μm) situated inside an FTIR spectrometer. The reduced IR absorbance at 1534 cm^{-1} yielded the amount of NBA consumed during the irradiation interval. The solution was then pumped back into the fused silica cell for the next irradiation. From the linear dependence of consumed NBA on the deposited light energy the quantum yield was calculated.

The setup used for the acquisition of the transient absorption data with probing in the near UV and visible range was described in detail elsewhere.[22] Therefore, here only the pertinent parameters will be summarized. A Ti:Sa laser amplifier system running at 775 nm with a repetition rate of 1 kHz (Clark, CPA 2001) served as the light source. Excitation light at 258 nm and 388 nm was generated from these pulses by second and third harmonic generation in BBO crystals, respectively. The beam size in the focal region, for both excitation wavelengths, was determined to be around 85 μm (FWHM). In the 258 nm experiment the energy of the pump pulses amounted to 300 nJ. In the 388 nm experiment pulse energy was attenuated to 400 nJ. Probe light was generated by continuum generation. A portion of the output of the laser system was focused onto an eccentrically moved CaF_2 crystal with a thickness of 5 mm. Its diameter in the focal region amounted to 40 μm. The relative polarization between pump and probe beam was set to the magic angle in both experiments. Pump and probe beam crossed in a wire guided jet.[22,28] The thickness of the sample solution in this jet amounted to ~150 μm. The jet was part of a flow system. The flow rate ensured exchange of the sample in between laser shots.

The total sample volume (~50 ml) was high enough to render contributions of accumulated photoproducts negligible. The same setup but with a different Ti:Sa amplifier system (Coherent, Libra F 1K HE 230) centered at 800 nm was used for some additional measurements. Since the amplifier exhibits a larger beam diameter, the branch for the probe pulses was adjusted using a lens telescope (fused silica, f_1 = 750 mm, f_2 = −200 mm). The focal diameter for the pump and probe beams amounted to 240 μm and 40 μm, respectively. The pump pulse energy equaled 1 μJ. A fused silica flow (pathlength of 200 μm) was used instead of the jet. All signals were corrected for the group delay dispersion of the probe light. The temporal reso lution of both instruments was ~200 fs.

The setup for the time resolved IR experiments was detailed elsewhere.[6,29] Here, pump pulses in the near UV were generated by second and third harmonic generation in BBO crystals of a portion of the output of a Ti:Sa laser amplifier system (Spectra Physics, Spitfire Pro 35F 1KXP). Since the wavelength of this system (810 nm) was different from the one used in the above mentioned experiments, the excitation light pulses also feature slightly different wavelengths. The energy of the 270 nm pump pulses amounted to 2 μJ. In the 405 nm experiment pulse ener gies of 240 nJ were used. The diameter at the focal region was 150 μm. The energy of the probe pulses in the mid IR amounted to 50 nJ in both experiments with a focal diameter of 100 μm. After passing the sample solution probe light was dispersed and detected in two spectrographs,[17] one for parallel polarization and one for perpendicular polarization. Magic angle data were calcu lated from these two data sets. The temporal resolution of the setup was 350 fs. The sample solution was pumped through the focal region in a home built flow cell. The one used for the 270 nm experiment featured a thickness of 90 μm, the concen tration of the sample solution amounted to 50 mM. In the 405 nm experiment a flow cell with a thickness of 100 μm was used and a sample concentration of 170 mM.

In all experiments described in the following, NBA from Merck (Germany) and tetrahydrofuran (Uvasol) from Merck (Germany) was used as received.

3. Results

3.1. Reaction quantum yields

As stated in the Introduction, the yield of the nitroso product exhibits no or only a weak dependence on the excitation wave length. For the solvent and excitation ranges employed, these yields were determined. For blue excitation (355 nm) the yield is 0.41 ± 0.02. For UV excitation (266 nm) its equals 0.48 ± 0.03. The values are in the range given in the literature.[23,24]

3.2. UV/Vis spectroscopy

In the spectral range of interest here NBA exhibits weak overlap ping absorption bands of nπ* character,[25,26] which become dis cernible for wavelengths smaller than ~400 nm (Fig. 1). Exciting NBA at 388 nm ought to address the lowest excited state of this molecule. Since the molar absorption coefficient ε_{388} is lower than 100 M^{-1} cm^{-1} concentrations of 48 mM were employed. Even for this high concentration the optical density at

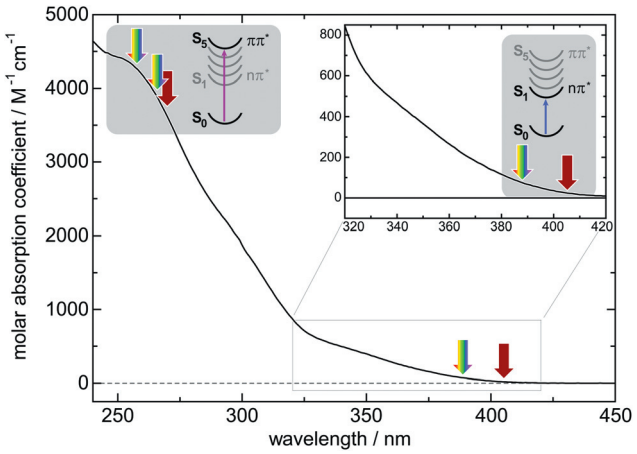

Fig. 1 Absorption spectrum (molar absorption coefficient *versus* wave length) of NBA dissolved in THF. Arrows mark the excitation wave lengths in the different pump probe experiments. The rainbow pattern represents the UV/Vis experiment, the dark red color stands for the IR experiment. The insert enlarges the tail of the NBA spectrum.

the excitation wavelength amounted to only 0.07. Since for this low molar absorption coefficient and optical density two photon excitation might contribute to the signal, its dependence on the pump intensity was investigated (see ESI, Fig. 1S and 2S†). For the given pulse duration and diameter at the sample the time traces start to deviate substantially in shape for pulse energies ≥1 μJ. Thus, for the data described in the following, pulse energies of 0.4 μJ were employed. When exciting a solution of NBA with femtosecond laser pulses centered at 388 nm, positive transient absorption changes are observed throughout the spectral range probed (Fig. 2, left). The negative dip at time zero and ~440 nm is due to femtosecond stimulated Raman scattering.[30–32] Around time zero a positive transient absorption spans the complete probe range and increases in magnitude for smaller wavelengths. After several 100 fs a band peaking at ~450 nm becomes discernible. It shifts to longer wavelengths and narrows on the 10 ps time scale. Afterwards a slight signal increase is observed before the band decays with a characteristic time of the order of nanoseconds.

For UV excitation the neat solvent THF exhibits strong signals around time zero due to the simultaneous absorption of one pump and one probe photon.[31] Further, two photon absorption of pump photons generate solvated electrons,[33] which cause longer lived signals. A concentration dependence detailed in the ESI (Fig. 3S and 4S†) shows that due to inner filter effects longer lived solvent contributions vanish for concentrations larger than 20 mM. At time zero higher concentrations of roughly 50 mM are required to suppress the solvent contribution. For 20 mM a larger spectroscopic range is accessible and this concentration was thus employed to determine time constants larger than 0.5 ps. For shorter time constants 50 mM data was relied on. For 258 nm excitation and delay times larger than a couple of picoseconds, a pattern similar to one for 388 nm is recorded (Fig. 2, right). For this excitation wavelength an upper singlet excited state (*cf.* Fig. 1 and ref. 25 and 26) is addressed. This excitation results in a transient absorption around time zero, which is stronger in relation to the signals recorded at later delay times in comparison to the one seen for 388 nm

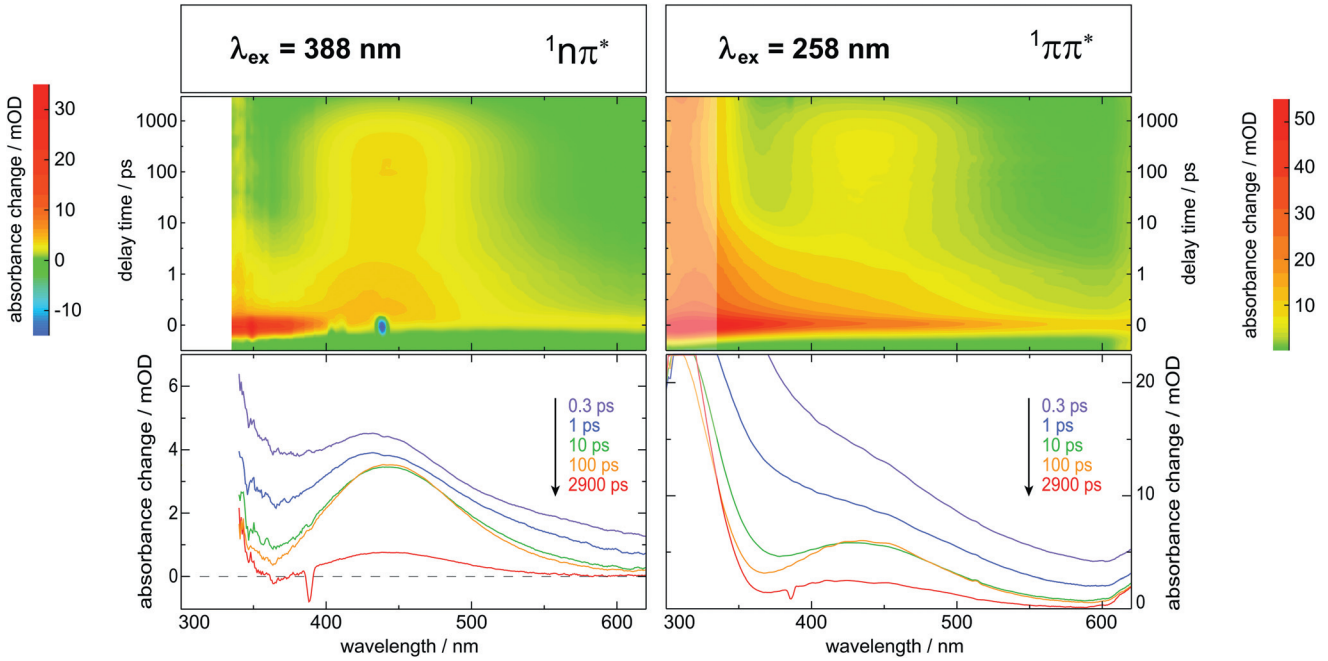

Fig. 2 UV/Vis transient absorption data of NBA dissolved in THF. In the upper contour representation large positive absorption changes are rep resented by red coloring. The time axis is linear up to 1 ps and logarithmic thereafter. In the lower panels transient spectra at indicated delay times are plotted. For the data on the left the femtosecond excitation pulse had a wavelength of 388 nm and was in resonance with the lowest excited state. In this experiment the NBA concentration amounted to 48 mM. Due to this high concentration no data could be recorded for probe wavelength smaller 350 nm. The graphs on the right represent data obtained for 258 nm excitation. The excitation pulse is in resonance with an upper singlet state. The concentration amounted to 20 mM. Due to differences in the excitation conditions the signal magnitudes cannot be compared directly.

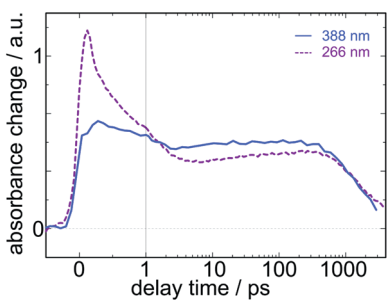

Fig. 3 Comparison of time traces for 388 nm and 266 nm excitation. In either case probe wavelength was equal to 450 nm close to the maximum of the ketene absorption. The concentration amounted to 48 mM. The traces were scaled to the same value at 1 ns.

excitation. Furthermore, the shifting and narrowing on the 10 ps time scale is more pronounced. For delay times larger than 10 ps the signatures for the two excitation wavelengths merge. A com parison of two time traces (Fig. 3) highlights this merging. The spectral coincidence and the nanosecond lifetime strongly suggest that for either excitation wavelength the ketene is formed. For UV excitation this was already proven by IR spec troscopy,[14,17] for blue excitation this will now be complemented.

3.3. IR spectroscopy

The tell tale stretching vibration at ~2100 cm^{-1} has often been used to identify transient ketenes,[34–36] in particular the one derived from NBA.[14,17,21,37] The results for UV excitation are thoroughly described in ref. 17 and are compared to the one for blue excitation in Fig. 4. For UV (270 nm) excitation the ketene band is visible ~0.5 ps after photo excitation. It is first centered around 2050 cm^{-1} and shifts to 2100 cm^{-1} within ~10 ps. After a slight increase on the 100 ps time scale the band decays within some nanoseconds. The blue (405 nm) experiment suffers from the very low molar absorption coefficient at the excitation wave length, which amounts to less than 50 M^{-1} cm^{-1} (*cf.* Fig. 1). This results in transient absorption signals more than an order of magnitude smaller than for UV excitation. Thus, for early delay times when the ketene band is expected to be broadened, the ketene signature cannot be distinguished from noise and non linear signals caused by the solvent. From ~10 ps onwards, however, the band is visible and exhibits a similar spectro temporal behavior as in the UV experiment. This gives clear evidence that for either excitation wavelength the ketene inter mediate is formed. At a delay time of 1 ps (for earlier time no value can be obtained for the blue set) the initial frequency shifts amount to 38 cm^{-1} and 26 cm^{-1}.

3.4. Data analysis

In a global analysis with a multi exponential trial function five exponentials with time constants τ_{1-5} and an offset were required to describe the UV data set.[17] Inspection of the blue data set show that here four exponentials and an offset suffice. The time constants and decay associated spectra (DAS) ΔA_i are compiled in Fig. 5. The two sets of time constants are except for the

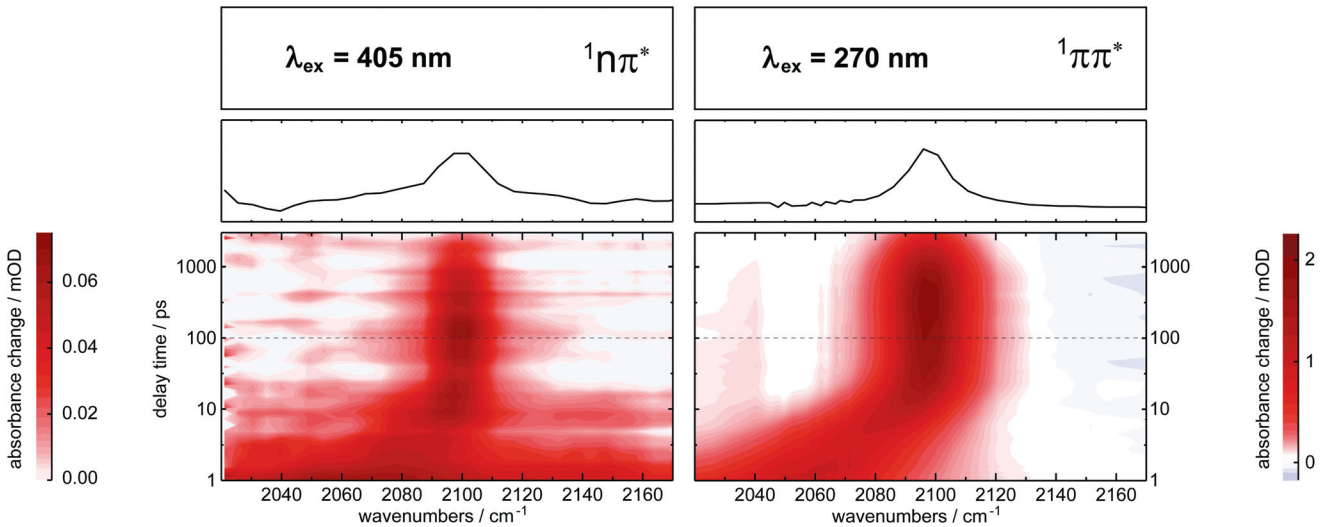

Fig. 4 Transient IR data for NBA dissolved in THF. The spectral range for IR probing is centered around 2100 cm^{-1} where the ketene functions are known to absorb. In the lower contour representation large positive absorption changes are represented by red coloring. In the panel above, the transi ent spectra 100 ps after excitation are plotted. For the data on the left the excitation wavelength was equal to 405 nm, on the right it was tuned to 270 nm. Due to differences in the excitation conditions the signal magnitudes cannot be compared directly.

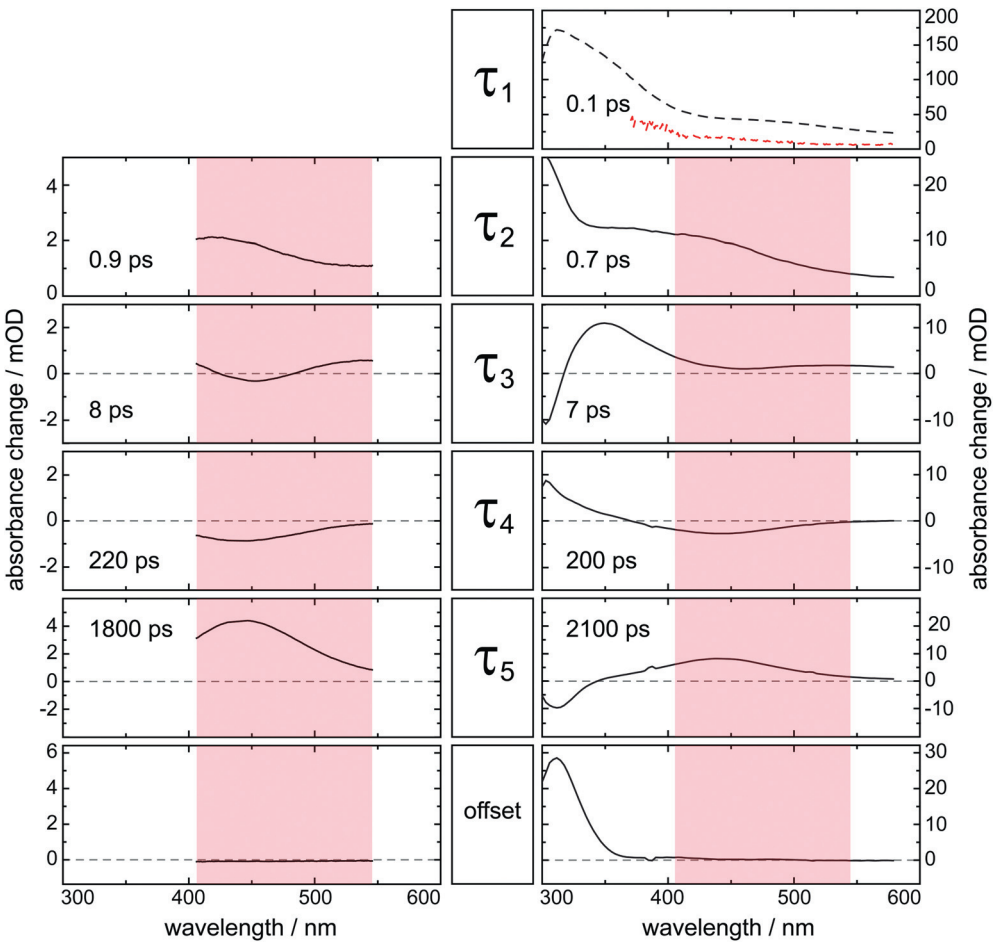

Fig. 5 Decay associated spectra obtained from a global analysis of the transient absorption data depicted in Fig. 2. Results for the 388 nm excitation are plotted on the left, those for the 258 nm excitation on the right. The 258 nm DAS plotted in black refer to a measurement utilizing a concentration of 20 mM. Since for this concentration the signal around time zero is perturbed by the solvent, for the DAS ΔA_1 we relied on a measurement with higher concentration (48 mM) (red dashed line). For details see text and ESI.†

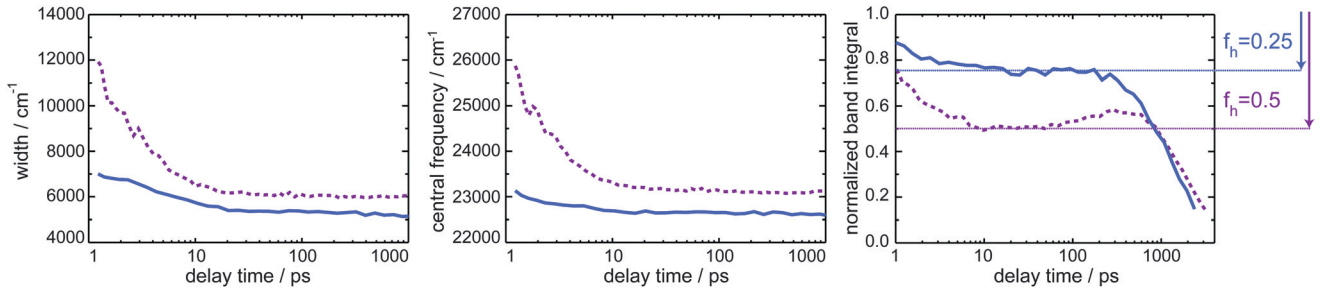

Fig. 6 Band shape analysis of the UV/Vis transient absorption data depicted in Fig. 2. Transient spectra at different delay times were subject to a fit by Gaussians, as described in the text. One Gaussian represents the Vis absorption band of the ketene. Its width (FWHM), central frequency, and band integral are plotted as a function of the delay time. The blue solid lines represent data for 388 nm excitation. The dashed violet line stands for 258 nm excitation. The band integrals were normalized to the value at ~0.5 ps. The fractions f_h reacting *via* the hot channel are marked.

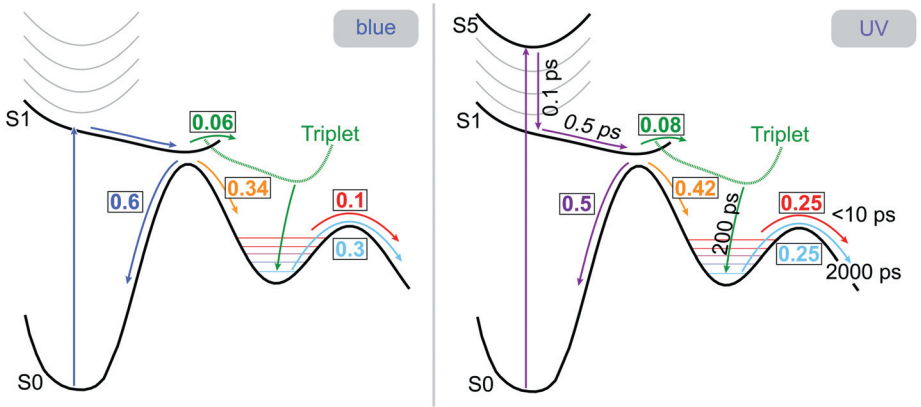

Fig. 7 Scheme summarizing the approximate branching ratios (numbers in boxes) for UV and blue excitation. Note that all values refer to the population of the initially excited state, which was set to one. For UV excitation the relevant rounded time constants are included, where applicable the same values apply for blue excitation.

missing τ_1 component in the blue set identical within error margin. (The rather high number of time constants requires a comment concerning their accuracy. An exhaustive search algorithm[38] yields typical error margins of ±30% for the time constants, which are mostly an order of magnitude apart from each other. Our "impression" is that the actual error margins are smaller. Other time resolved techniques (fluorescence and IR) which selectively detect only some of the time constants afford values which deviate by less than 30% (see ref. 17).) In the spectral range for which both data sets were analyzed the DAS are also very similar. This applies to the shape of the DAS for one time constant τ_i as well as *relative* amplitudes note that the absolute amplitudes must not be compared since the excitation conditions were not identical. Two differences should be noticed. The DAS ΔA_3 is negative around 450 nm for blue excitation whereas for the UV data it is positive (but exhibits a minimum). Relative to the other DAS the ΔA_5 spectrum is higher by a factor of ~2 for the blue experiment.

As the following analysis will show, these differences can be attributed to the amount of vibrational excitation of the ketene. Vibrational excitation is known to shift and broaden UV/Vis absorption bands.[5,39] To quantify these band distortions we here adopt the same approach as in ref. 17. The transient spectra (*versus* a wavenumber axis) at a given delay time are fitted by Gaussians and the parameters of these Gaussians are plotted *versus* the delay time (Fig. 6). A sum of two Gaussians was used.[17] One Gaussian to parametrize the band centered around 450 nm ascribed to the ketene and an "auxiliary" one for a second band in the near UV. This band can either be due to a higher excited state of the ketene or due to the product formed during the ketene decay. Within ~10 ps the parameters describing the Gaussians approach a constant value. This constant value is slightly different for the two excitation wavelengths. These differences might be due to the fact that the "auxiliary" band is better defined for the UV data, the spectral coverage is larger there. While the time constants for the vibrational relaxation are similar for both excitation wavelengths, the shifts and widths at time zero are larger for UV excitation. The maximal displacements for the width are 6000 (UV) and 900 cm^{-1} (blue) and those for the central frequency are 2800 (UV) and 500 cm^{-1} (blue). Differences are also observed for the band integrals. For blue excitation the integral decreases by a fraction f_h of ~0.25 after the first 10 ps whereas for UV excitation the fraction f_h is around 0.5. For either wavelength a slight increase on the 100 ps time scale and a decay within some nanoseconds is seen.

4. Discussion

We first briefly reiterate the assignment of the kinetic components for the 260 nm experiment given in ref. 17 (*cf.* Fig. 7,

Scheme 1). The time constant $\tau_1 \approx 0.1$ ps was associated with the decay of the ππ* singlet state and the constant $\tau_2 = 0.7$ ps with the decay of an nπ* state. The assignment was based on the fact that very similar time constants were measured in a femto second fluorescence experiment.[16] The time constant $\tau_3 = 7$ ps matches the time scale of the shift of the ketene vibration observed in the IR experiment (Fig. 4). This and the shape of the DAS ΔA_3 allow to associate this time constant with vibrational cooling of the nascent ketene. Around the absorption peak of the ketene at 440 nm the DAS ΔA_4 is negative and adopts the shape of the ketene band. Thus, an additional rise of the ketene popu lation occurs with a time constant of $\tau_4 = 200$ ps. With the time constant $\tau_5 = 2000$ ps the ketene finally decays (positive band in the DAS ΔA_5 peaking at 440 nm) and the kinetic successor of the ketene rises (negative band peaking at 310 nm). The DAS ΔA_∞ represents the spectrum of this successor. Former investi gations[17] showed that this successor is not identical to the nitroso photo product. It was proposed that a lactone is respon sible for that band.[17]

A kinetic scheme incorporating these spectroscopic findings looks as follows (Fig. 7, Scheme 1). Excitation to an excited singlet state of ππ* character induces ultrafast (~100 fs) IC pro cesses populating a lower or the lowest nπ* singlet state. Three kinetic processes contribute to the decay of this state. (i) IC par tially recovers the NBA ground state. Femtosecond IR exper iments give evidence for this recovery and its yield of ~0.5 (50%).[17] Alternatively the ketene intermediate is formed *via* hydrogen transfer (ii) and ISC to the triplet state occurs (iii). Hydrogen transfer of the triplet excited NBA results in a bi radical. Its recombination (time constant $\tau_4 = 200$ ps) is respon sible for a further rise of the ketene population. The vibrationally relaxed ketene decays within $\tau_5 = 2000$ ps to eventually trans form into the nitroso product. The fast phase (<10 ps) of the ketene decay which the band shape analysis reveals (Fig. 6) is due to the initial vibrational excitation of the ketene. We will refer to that as the "hot channel" below.

When tuning the excitation to ~400 nm and thereby addres sing the lowest nπ* singlet state the τ_1 process "vanishes". This lends very strong support to the above assignment of this process to IC between excited singlet states. The other time constants and DAS are very similar to the ones of the UV experiment. The two differences mentioned above the negative contribution in the DAS ΔA_3 and the higher relative amplitude of the DAS ΔA_5 can both be related to the lower vibrational excitation. The ΔA_3 spectrum "summarizes" two effects. Spectral narrowing and shifting of the ketene band due to vibrational relaxation and decay of the ketene *via* the hot channel. Narrowing and shifting translates into a DAS with a negative contribution at the peak of a band and positive ones at its wings, as seen in the blue data. A decay of a species results in positive contributions. Since for UV excitation the fraction of the ketene population f_h decaying *via* the hot channel is higher, the signature for narrowing and shifting sits on top of a (higher) positive background. The frac tion of ketene population lost *via* the hot channel of course reduces the amplitude of the slow channel represented by the DAS ΔA_5. When computing a corrected DAS $\Delta A_{5,c}$ according to

$$\Delta A_{5,c} = \frac{\Delta A_5}{1 - f_h} \quad (1)$$

the relative amplitudes of the DAS $\Delta A_{2,4,5c}$ are very close to each other for the two excitation wavelengths. With this correction the triplet contribution f_t to the ketene formation is given by

$$f_t = \frac{|\Delta A_4(440\text{ nm})|}{\Delta A_{5,c}(440\text{ nm})}. \quad (2)$$

The amplitudes were evaluated for the peak of the ketene band at 440 nm. The value obtained for UV excitation is 0.16 and very close to the blue one (0.15). For the computation of these values it was assumed that for the triplet pathway no hot channel exists. Based on the time resolved data it is not possible to compare the overall quantum yield for the ketene formation. However, it has been shown that the ketene trans forms quantitatively into the final nitroso product.[14,20] As the nitroso yield only weakly depends on the excitation wave length, this also has to apply to the ketene yield. Thus, not only does the same kinetic branching occur for both wavelengths, but also the relative contributions of the different channels are very close.

The pronounced differences observed for the hot channels can be related to the respective energies deposited in the molecule. A simple model detailed in ref. 17 can reproduce this observation. The rate constant k of the ketene decay is hereby assumed to obey Arrhenius' law

$$k = k_0 \exp\left(-\frac{E_a}{k_b T}\right) \quad (3)$$

with the activation energy E_a and the pre exponential factor k_0. After vibrational relaxation the temperature equals room temp erature (T_0) and the rate constant k equals $1/\tau_5$. In a crude approximation the vibrational excitation is parametrized by a time dependent temperature $T(t)$. The initial temperature increase ΔT is computed using the photon energy E_{ph}, the energy of ketene intermediate E_k with respect to NBA and the vibrational contribution to the heat capacity $c_v(T)$. The last two quantities were obtained from density functional computations. The expression reads:

$$E_{ph} - E_k = \int_{T_0}^{T_0+\Delta T} c_v(T)\,dT \quad (4)$$

For UV excitation the resulting increase ΔT equals 1400 K, for blue excitation it amounts to 900 K. As the band shape analysis conducted here (Fig. 6) and earlier has shown,[17] the molecules cool down to room temperature within less than ~10 ps. For the UV experiment the shift $\Delta\tilde{\nu}$ of the ketene band in the IR was used as an indicator for the vibrational excitation. It was assumed that this indicator scales linearly with the temperature. In the present comparison between UV and blue excitation it was observed that at 1 ps after photo excitation the respective shifts amounted to 38 (UV) and 26 cm^{-1} (blue). This lends support to the assumed linear scaling: 38 cm^{-1}/26 cm^{-1} ≈ 1400 K/900 K. We note, however, that such a linear dependence is not observed when comparing the respective parameters for UV/Vis detection. This discrepancy is presently investigated. In ref. 17 the normal ized time dependence of the frequency shift $\Delta\tilde{\nu}$ was used to

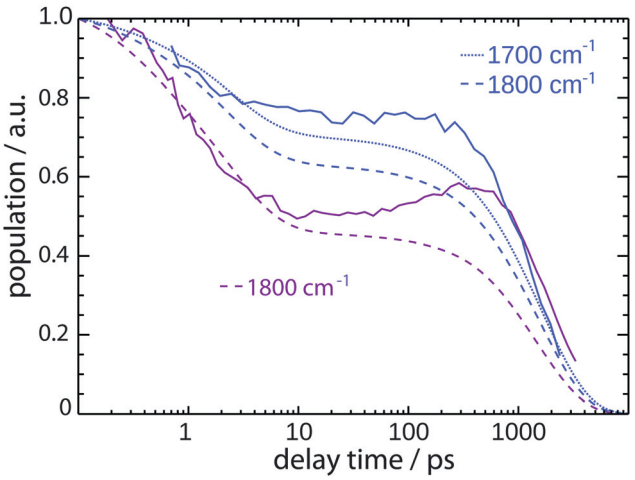

Fig. 8 Experimental band integrals representing the ketene population (solid lines) in comparison with simulations (dashed and dotted lines) modeling the impact of the vibrational excitation on the kinetics (see text). The blue solid (violet) lines represent data for 388 nm (258 nm) excitation.

parametrize the vibrational cooling. This parameter $n_f(t)$ was subject to a bi exponential fit. Its result is given by

$$n_f(t) = 0.4\exp\left(-\frac{t}{0.3\ \text{ps}}\right) + 0.6\exp\left(-\frac{t}{6\ \text{ps}}\right). \quad (5)$$

With this input the time dependent population of the ketene $p(t)$ can be computed according to

$$p(t) = \exp\left(-k_0 \int_0^t \frac{E_a}{k_b(T_0 + \Delta T n_f(t))}\, dt\right). \quad (6)$$

(In ref. 17 the upper boundary of the integral has erroneously been designated with ∞ instead of t. For the computations the correct boundary was used.) For an activation energy E_a of 1800 cm^{-1} and a pre exponential factor k_0 of 1/(0.35 ps) this model is a good approximation for the experimental behavior for UV excitation (Fig. 8). The respective band of the UV/Vis data serves as an experimental measure for the population. The model reproduces the temporal characteristics of the hot channel as well as the fraction f_h reacting *via* this channel. The experimental time trace deviates from the computed one on the 100 ps time scale. The rise component seen in the experiment is due to ketene formation *via* the triplet state not incorporated in the model. To model the ketene decay for blue excitation identical parameters were employed, except for a lower initial temperature rise ΔT. As in the experimental time trace, the lower temperature reduces the fraction f_h. In the experiment the reduction is more pronounced than in the simulation. By only slightly changing the activation energy E_a to 1700 cm^{-1} a reasonable agreement is achieved.

Comparison of the transient signatures for both excitations has shown that NBA obeys Kasha's rule very well. No indications for state selective photochemistry are observed. The experiments have shown that one prerequisite for Kasha's rule is fulfilled. IC processes between upper excited states are ultrafast they occur within 100 fs or less. Taking into account that UV excitation is in resonance with the S_5 state whereas the blue excitation addresses the S_1 [26] at least formally several IC processes occur within ~100 fs. The quantum chemistry computations on the MS CASPT2/CASSCF level[18] have located various CIs mediating transitions between the S_5 state and lower singlet states. Yet, a path connecting the Franck Condon region of the of S_5 state with the nπ* state has not been optimized yet. The second prerequisite for Kasha's rule is not fulfilled here. The hydrogen transfer yielding the ketene is faster than vibrational relaxation. This implies that for UV excitation ~10 000 cm^{-1} of additional vibrational excitation are available compared to blue excitation. Still, the lifetime of the nπ* state and yields of the channels contributing to its decay are only weakly affected. This suggests that the contributing processes are activationless. The computations[18] indeed show that a barrierless path connecting the nπ* state and the ketene ground state exists. This necessitates a crossing or CI between excited and ground state surface. There branching can occur and a part of the population reforms the ground state and a part the ketene. Due to this branching the recovery of the ground state *and* the ketene formation are expected to be activationless. Classical dynamics simulations incorporating non adiabatic effects for nπ* excitation[27] yield a branching ratio of 0.7/0.3 (ground state recovery *versus* ketene formation). Experimentally, at first glance the ratio is 0.6/0.4. Considering that a fraction of ~0.2 of the overall ketene amount is formed *via* the triplet, the singlet branching which is relevant for the simulations is 0.65/0.35, very close to the value obtained in the simulations. As reported here there is a *slight* increase in the photochemical yield for UV excitation. This might be caused by a weak effect on the branching ratio. Such ratios are expected to depend on the momentum with which the CI is approached. For UV excitation one would expect a larger momentum.

Despite the fact that fast spin converting processes deplete the lowest excited singlet state, ISC yielding a triplet excited state occurs with a yield of the order of 0.1. This study has unequivocally shown that the initial state for the ISC is of nπ* character. Based on El Sayed rules[2,40] the triplet state accessed ought to be a ππ*. The short triplet lifetime of nitrobenzene derivatives,[41,42] however, suggest that their lowest triplet state is of nπ* character. ISC should thus be followed by an IC process within the triplet manifold. Such a behavior was also suggested for nitrobenzene[43] and nitrated polyaromatic compounds.[44]

Kasha's rule is based on the assumptions that non radiative processes between upper excited states and vibrational relaxation are faster than radiative and/or photochemical processes. For NBA the first assumption seems to apply despite that the fact that the photochemical reaction occurs on the time scale of several 100 fs the internal conversion between upper excited states is even faster. The second assumption is not valid here. Vibrational relaxation is slower than the initial hydrogen transfer. However, this only very slightly affects the branching ratios and thereby the overall photochemical yield. It has a strong impact on the *kinetics* of the ketene decay. Varying the wavelength changes the degree of vibrational excitation and thereby the fraction which decays *via* the hot channel. However, since no competing channel seems to exist no effect on the *yield* is observed.

Acknowledgements

This work was supported by the Deutsche Forschungsgemeinschaft (projects GI 349/1 2, GI 349/4 1, and GI 349/5 1).

We thank Wolfgang Zinth for the IR data recorded in this laboratory.

References

1 M. Kasha, Characterization of electronic transitions in complex molecules, *Discuss. Faraday Soc.*, 1950, **9**, 14 19.
2 P. Klan and J. Wirz, *Photochemistry of Organic Compounds. From Concepts to Practice*, Wiley, Chichester, 2009.
3 R. Englman and J. Jortner, Energy gap law for radiationless transitions in large molecules, *Mol. Phys.*, 1970, **18**, 145 164.
4 A. Seilmeier and W. Kaiser, Ultrashort intramolecular and intermolecular vibrational energy transfer of polyatomic molecules in liquids, in *Topics in Applied Physics*, ed. W. Kaiser, Elsevier-Verlag, Amsterdam, 1993, ch. 7, vol. 60, pp. 279 317.
5 S. A. Kovalenko, S. Schanz, H. Hennig and N. P. Ernsting, Cooling dynamics of an optically excited molecular probe in solution from femtosecond broadband transient absorption spectroscopy, *J. Chem. Phys.*, 2001, **115**, 3256 3273.
6 T. Schrader, A. Sieg, F. Koller, W. Schreier, Q. An, W. Zinth and P. Gilch, Vibrational relaxation following ultrafast internal conversion: comparing IR and Raman probing, *Chem. Phys. Lett.*, 2004, **392**, 358 364.
7 N. Tamai and H. Miyasaka, Ultrafast dynamics of photochromic systems, *Chem. Rev.*, 2000, **100**, 1875 1890.
8 A. H. Zewail, Femtochemistry: atomic-scale dynamics of the chemical bond, *J. Phys. Chem. A*, 2000, **104**, 5560 5694.
9 N. J. Turro, V. Ramamurthy and J. C. Scaiano, *Principles of Molecular Photochemistry. An Introduction*, University Sciences Books, Sausalito, California, 2009.
10 T. Fujino, S. Yu. Arzhantsev and T. Tahara, Femtosecond time-resolved fluorescence study of photoisomerization of *trans*-azobenzene, *J. Phys. Chem. A*, 2001, **105**, 8123 8129.
11 T. Cordes, S. Malkmus, J. A. DiGirolamo, W. J. Lees, A. Nenov, R. de Vivie-Riedle, M. Braun and W. Zinth, Accelerated and efficient photochemistry from higher excited electronic states in fulgide molecules, *J. Phys. Chem. A*, 2008, **112**, 13364 13371.
12 R. S. Becker, E. Dolan and D. E. Balke, Vibronic effects in photochemistry competition between internal conversion and photochemistry, *J. Chem. Phys.*, 1969, **50**, 239 245.
13 P. L. Gentili, E. Danilov, F. Ortica, M. A. J. Rodgers and G. Favaro, Dynamics of the excited states of chromenes studied by fast and ultrafast spectroscopies, *Photochem. Photobiol. Sci.*, 2004, **3**, 886 891.
14 S. Laimgruber, W. J. Schreier, T. Schrader, F. Koller, W. Zinth and P. Gilch, The photochemistry of *o*-nitrobenzaldehyde as seen by femtosecond vibrational spectroscopy, *Angew. Chem., Int. Ed.*, 2005, **44**, 7901 7904.
15 S. Laimgruber, T. Schmierer, P. Gilch, K. Kiewisch and J. Neugebauer, The ketene intermediate in the photochemistry of *ortho*-nitrobenzaldehyde, *Phys. Chem. Chem. Phys.*, 2008, **10**, 3872 3881.
16 B. Heinz, T. Schmierer, S. Laimgruber and P. Gilch, Excited state processes of nitrobenzaldehydes probed by ultrafast fluorescence and absorption spectroscopy, *J. Photochem. Photobiol., A*, 2008, **199**, 274 281.
17 T. Schmierer, W. J. Schreier, F. O. Koller, T. E. Schrader and P. Gilch, Impact of vibrational excitation on the kinetics of a nascent ketene, *Phys. Chem. Chem. Phys.*, 2009, **11**, 11596 11607.
18 A. Migani, V. Leyva, F. Feixas, T. Schmierer, P. Gilch, I. Corral, L. Gonzalez and L. Blancafort, Ultrafast irreversible phototautomerization of *o*-nitrobenzaldehyde, *Chem. Commun.*, 2011, **47**, 6383 6385.
19 M. V. George and J. C. Scaiano, Photochemistry of *o*-nitrobenzaldehyde and related studies, *J. Phys. Chem.*, 1980, **84**, 492 496.
20 R. W. Yip and D. K. Sharma, The reactive state in the photo-rearrangement of *ortho*-nitrobenzaldehyde, *Res. Chem. Intermed.*, 1989, **11**, 109 116.
21 M. L. Donten, P. Hamm and J. VandeVondele, A consistent picture of the proton release mechanism of oNBA in water by ultrafast spectroscopy and *Ab Initio* molecular dynamics, *J. Phys. Chem. B*, 2011, **115**, 1075 1083.
22 S. Laimgruber, H. Schachenmayr, B. Schmidt, W. Zinth and P. Gilch, A femtosecond stimulated Raman spectrograph for the near ultraviolet, *Appl. Phys. B: Lasers Opt.*, 2006, **85**, 557 564.
23 H. J. Kuhn, S. E. Braslavsky and R. Schmidt, Chemical actinometry, *Pure Appl. Chem.*, 2004, **76**, 2105 2146.
24 E. S. Galbavy, K. Ram and C. Anastasio, 2-Nitrobenzaldehyde as a chemical actinometer for solution and ice photochemistry, *J. Photochem. Photobiol., A*, 2010, **209**, 186 192.
25 V. Leyva, I. Corral, T. Schmierer, B. Heinz, F. Feixas, A. Migani, L. Blancafort, P. Gilch and G. Leticia, Electronic states of *o*-nitrobenzaldehyde: a combined experimental and theoretical study, *J. Phys. Chem. A*, 2008, **112**, 5046 5053.
26 V. Leyva, I. Corral, T. Schmierer, P. Gilch and L. Gonzalez, A comparative analysis of the UV/Vis absorption spectra of nitrobenzaldehydes, *Phys. Chem. Chem. Phys.*, 2011, **13**, 4269 4278.
27 V. Leyva, I. Corral, F. Feixas, A. Migani, L. Blancafort, J. Gonzalez-Vazquez and L. Gonzalez, A non-adiabatic quantum-classical dynamics study of the intramolecular excited state hydrogen transfer in *ortho*-nitrobenzaldehyde, *Phys. Chem. Chem. Phys.*, 2011, **13**, 14685 14693.
28 M. J. Tauber, R. A. Mathies, X. Y. Chen and S. E. Bradforth, Flowing liquid sample jet for resonance Raman and ultrafast optical spectroscopy, *Rev. Sci. Instrum.*, 2003, **74**, 4958 4960.
29 T. E. Schrader, W. J. Schreier, T. Cordes, F. O. Koller, G. Babitzki, R. Denschlag, C. Renner, M. Loweneckt, S. L. Dong, L. Moroder, P. Tavan and W. Zinth, Light-triggered beta-hairpin folding and unfolding, *Proc. Natl. Acad. Sci. U. S. A.*, 2007, **104**, 15729 15734.
30 S. Kovalenko, A. Dobryakov, J. Ruthmann and N. Ernsting, Femtosecond spectroscopy of condensed phases with chirped supercontinuum probing, *Phys. Rev. A: At., Mol., Opt. Phys.*, 1999, **59**, 2369 2384.
31 M. Lorenc, M. Ziolek, R. Naskrecki, J. Karolczak, J. Kubicki and A. Maciejewski, Artifacts in femtosecond transient absorption spectroscopy, *Appl. Phys. B: Lasers Opt.*, 2002, **74**, 19 27.
32 P. Kukura, D. W. McCamant and R. A. Mathies, Femtosecond stimulated Raman spectroscopy, *Annu. Rev. Phys. Chem.*, 2007, **58**, 461 488.
33 I. B. Martini, E. R. Barthel and B. J. Schwartz, Mechanisms of the ultrafast production and recombination of solvated electrons in weakly polar fluids: comparison of multiphoton ionization and detachment via the charge-transfer-to-solvent transition of Na- in THF, *J. Chem. Phys.*, 2000, **113**, 11245 11257.
34 Y. Chiang, A. V. Fedorov, A. J. Kresge, L. Onyido and T. T. Tidwell, Hydration of phenylketene revisited: a counter-intuitive result, *J. Am. Chem. Soc.*, 2004, **126**, 9382 9386.
35 A. V. Fedorov, E. O. Danilov, A. G. Merzlikine, M. A. J. Rodgers and A. C. Neckers, Application of time-resolved step-scan Fourier transform infrared spectroscopy to photochemical mechanistic investigations of alkyl phenylglyoxylates, *J. Phys. Chem. A*, 2003, **107**, 3208 3214.
36 D. Wolpert, M. Schade and T. Brixner, Femtosecond midinfrared study of the photoinduced Wolff rearrangement of diazonaphthoquinone, *J. Chem. Phys.*, 2008, **129**, 094504.
37 S. Kuberski and J. Gebicki, Evidence for a ketene intermediate in the photochemical transformation of matrix-isolated *o*-nitrobenzaldehyde, *J. Mol. Struct.*, 1992, **275**, 105 110.
38 H. Satzger and W. Zinth, Visualization of transient absorption dynamics towards a qualitative view of complex reaction kinetics, *Chem. Phys.*, 2003, **295**, 287 295.
39 T. Elsaesser and W. Kaiser, Vibrational and vibronic relaxation of large polyatomic-molecules in liquids, *Annu. Rev. Phys. Chem.*, 1991, **42**, 83 107.
40 M. A. El-Sayed, Spin orbit coupling and the radiationless processes in nitrogen heterocyclics, *J. Chem. Phys.*, 1963, **38**, 2834 2838.
41 R. W. Yip, D. K. Sharma, R. Giasson and D. Gravel, Picosecond excited-state absorption of alkyl nitrobenzenes in solution, *J. Phys. Chem.*, 1984, **88**, 5770 5772.
42 M. Takezaki, N. Hirota and M. Terazima, Nonradiative relaxation processes and electronically excited states of nitrobenzene studied by picosecond time-resolved transient grating method, *J. Phys. Chem. A*, 1997, **101**, 3443 3448.
43 M. Takezaki, N. Hirota and T. Terazima, Relaxation of nitrobenzene from Excited Singlet State, *J. Chem. Phys.*, 1998, **108**, 4685 4686.
44 E. F. Plaza-Medina, W. Rodriguez-Cordoba and J. Peon, Role of upper triplet states on the photophysics of nitrated polyaromatic compounds: S(1) lifetimes of singly nitrated pyrenes, *J. Phys. Chem. A*, 2011, **115**, 9782 9789.